Journal of The Electrochemical Society

OPEN ACCESS

Li_2NiO_2F a New Oxyfluoride Disordered Rocksalt Cathode Material

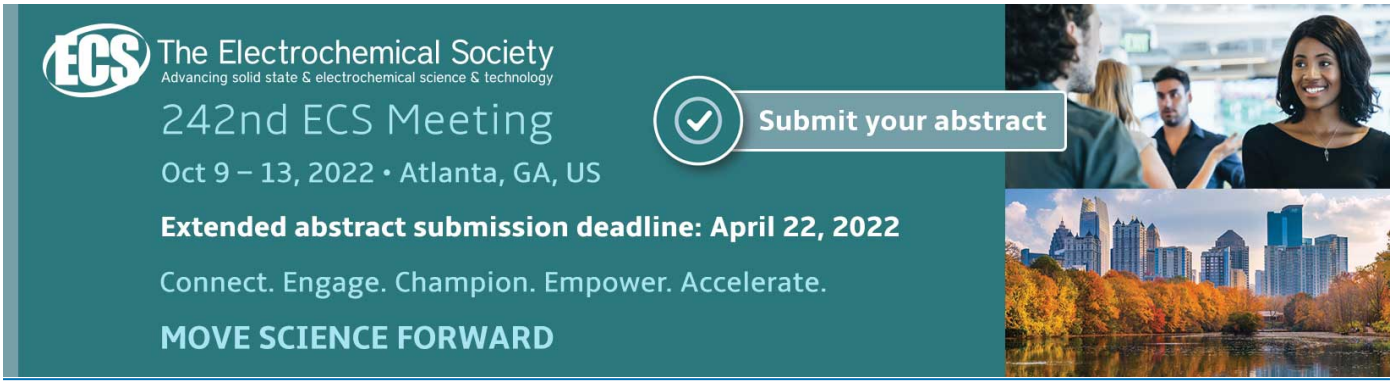

Journal of The Electrochemical Society, 2021 **168** 080521

Li_2NiO_2F a New Oxyfluoride Disordered Rocksalt Cathode Material

Xiaoyu Xu,[1,2,3,4] Liquan Pi,[1,2,3,4] John-Joseph Marie,[1,2,3,4] Gregory J. Rees,[1,2,3,4] Chen Gong,[1,2,3,4] Shengda Pu,[1,2,3,4] Robert A. House,[1,2,3,4] Alexander W. Robertson,[1,2,3,4] and Peter G. Bruce[1,2,3,4,*,z]

[1]*Departments of Materials, University of Oxford, Oxford, United Kingdom*
[2]*Department of Chemistry, University of Oxford, Oxford, United Kingdom*
[3]*The Henry Royce Institute, University of Oxford, Oxford, United Kingdom*
[4]*Faraday Institution, Harwell Campus, Didcot, United Kingdom*

Lithium-rich disordered rocksalts such as $Li_{1.3}Nb_{0.3}Mn_{0.4}O_2$ and Li_2MnO_2F are being investigated as high energy density cathodes for next generation Li-ion batteries. They can support the (de) lithiation of lithium ions over large compositional ranges while preserving the same overall structure. Here, we present a new Ni-rich oxyfluoride cathode, Li_2NiO_2F, with a disordered rocksalt structure. Li_2NiO_2F and can deliver a discharge capacity of 200 mAh g^{-1} at an average voltage of 3.2 V.
 [DOI: 10.1149/1945-7111/ac1be1]

Manuscript submitted April 12, 2021; revised manuscript received July 30, 2021. Published August 16, 2021.

Supplementary material for this article is available online

Finding new, high energy density cathode materials which are free from Co is crucial for the development of next generation batteries. In the race to eliminate Co from Li-ion batteries, there is a great effort underway to commercialize Ni-rich layered cathodes based on the composition $LiNiO_2$, however, these materials suffer from layer stacking changes and structural instability at high voltages. Recently, researchers have been looking beyond conventional layered cathodes towards disordered rocksalt materials which are able to retain crystal structure stability over large composition ranges. Cation disordered oxides such as $Li_4Mn_2O_5$,[1] $Li_{1.25}Nb_{0.25}Mn_{0.5}O_2$,[2] and $Li_{1.2}Ti_{0.4}Mn_{0.4}O_2$[3] are all capable of delivering reversible capacities in excess of 300 mAh g^{-1}. Despite the random distribution of transition metal (TM) and lithium ions among the cation sites, a large fraction of the Li-ions can still diffuse readily through the structure.[4,5] Beyond the oxide compounds, mixed anion oxyfluorides are also being investigated. The first reports of Li_2VO_2F in 2015 made by ball-milling[6] have since inspired others to synthesise a range of disordered rocksalt oxyfluoride cathodes materials with similar compositions, including Li_2MnO_2F,[7,8] Li_2FeO_2F,[9] Li_2TiO_2F,[10] Li_2MoO_2F[11] and those with two or more transition metals such as $Li_{1.171}Mn_{0.343}V_{0.486}O_{1.8}F_{0.2}$,[12] $Li_2Mn_{2/3}Nb_{1/3}O_2F$ and $Li_2Mn_{1/2}Ti_{1/2}O_2F$[13] many of which also exceed 300 mAh g^{-1} capacities at average voltages around 3 V.

The high capacities and stability of the disordered rocksalt structure inspired us to investigate the Ni-rich disordered rocksalt Li_2NiO_2F, to investigate whether some of the issues with $LiNiO_2$ could be avoided. A LiF-NiO composite fabricated by mechanical milling was already reported by Kobayashi et al. and showed promising electrochemical performance using mainly $Ni^{2+/3+}$ redox.[14] Other Ni^{2+}-containing rocksalts such as $Li_{1.3}Nb_{0.43}Ni_{0.27}O_2$ and $Li_{1.19}Ni_{0.59}Nb_{0.22}O_{1.46}F_{0.54}$ have also been demonstrated.[15,16] Li_2NiO_2F, which is free from inactive d^0 transition metals, offers the possibility to access high capacities supported by the $Ni^{3+/4+}$ redox couple which is generally higher voltage than $Fe^{3+/4+}$, $V^{3+/4+}$ or $Mn^{3+/4+}$ making it a suitable choice to target high energy densities. This compound is also Li-rich allowing access to the O-redox couple which may provide even higher capacities than $LiNiO_2$.

Here, we report the synthesis and electrochemical investigation of Li_2NiO_2F, with a disordered rocksalt structure and Ni in the +3 oxidation state. Capacity on the first charge to 4.8 V is 300 mAh g^{-1}, of which 200 mAh g^{-1} is recovered on subsequent discharge to 2.0 V. The average voltage on discharge is 3.2 V. Oxygen loss occurs on charge and Ni is reduced beyond 3+ on discharge. This study extends the family of Li_2TMO_2F oxyfluoride compounds to include TM = Ni^{3+}.

Experimental Methods

Synthesis.—Li_2NiO_2F was prepared by grinding together single-phase $LiNiO_2$ and commercial LiF (Aldrich, 99.99%) in the molar ratio 1:1 in an argon-filled glovebox. The mixture was then placed in a sealed zirconia jar of 20 cm^3 internal volume and ball milled at 750 rpm for 12 h in a Fritsch Pulverisette 7 planetary ball mill. The mass ratio between the powder and the balls was 1:30. The precursor $LiNiO_2$ was synthesised by mixing $LiNO_3$ (Aldrich, 99.99%) and $NiCO_3$ (Aldrich, 99.9%) in the molar ratio 1:1 in the glove box. A cold pressed pellet of the ground starting materials was then contained in an alumina boat inside a predried silica tube. The tube was heated to 650 °C under O_2 atmosphere at a rate of 2 °C min^{-1} and then held at 650 °C for 15 h before ramping back to room temperature at a rate of 2 °C min^{-1}. All samples were stored in an Ar-filled glove box (O_2/H_2O < 0.1 ppm) until further characterization.

Material characterization.—Powder X-ray diffraction (XRD) was carried out using a Rigaku SmartLab X-ray powder diffractometer equipped with a 9 kW Cu anode. GSAS Suite software was used to perform Rietveld refinements on powder X-ray diffraction data.

Elemental ratio of Li:Ni was determined through the analysis of Inductively Coupled Plasma - Optical Emission Spectroscopy (ICP-OES) using a Perkin-Elmer Optima 8000 ICP-OES. The ball-milled target product was first dissolved into 2% HNO_3. It was diluted to the concentration (1:200) that can be interpolated from available standard solutions with known molarity. The diluted samples were then loaded into the ICP instrument for analysis. For cycled materials, 10 wt% Al_2O_3 was added to the electrode as a constant internal reference and the Ni/Al ratio was measured to determine the Ni content in Li_2NiO_2F.

The morphology of the sample was characterized by a Zeiss Merlin analytical scanning electron microscope (SEM). Annular-dark field scanning transmission electron microscopy (ADF-STEM)

*Electrochemical Society Member.
[z]E-mail: peter.bruce@materials.ox.ac.uk

images were collected with JEOL ARM 200 F operated at a voltage of 200 kV.

Solid-state nuclear magnetic resonance (NMR) analysis was carried out at room temperature (298.15 K) on a Bruker Avance III HD 9.45 T spectrometer, operating at a Larmor frequency of ($\nu_0[^{19}F] =$) 376.6 MHz and ($\nu_0[^{6}Li] =$) 155.5 MHz. The data were obtained under magic angle spinning frequency ($V_R =$) of 37037 Hz ($\tau = 27\ \mu s$) using a 1.9 mm Bruker probe-head. The spectra were recorded using a Hahn echo ($\pi/2$-τ-π-τ) sequence. The respective chemical shift ranges were referenced against pure LiF powder ($\delta_{iso}(^{19}F) = -204$ ppm and $\delta_{iso}(^{6}Li) = -1$ ppm).

Operando electrochemical mass spectrometry (OEMS) was used in this work to probe evolution of O_2 gas from the Li_2NiO_2F cathode. A custom-made electrochemical cell with gas inlet and outlet ports was connected to a Thermo Fischer quadrupole mass spectrometer via sealed tubing. Turbomolecular pump (Pfeiffer Vacuum) and mass-flow controllers (Bronkhorst) were used to control the flowing rate of Ar gas in the cell.

Ni K-edge hard X-ray absorption near edge structure (XANES) experiments were performed at beamline B18 at the Diamond Light Source, Harwell, U.K. This beamline has a wide energy range (2.05 −35 keV) and is equipped with a double-crystal monochromator containing two pairs of crystals, Si (111) and Si (311), optimized for quick EXAFS measurements.[17] The data were collected in transmission mode and the intensities of the incident and transmitted beams were measured via gas filled ionization chambers. Two or three scans were collected for each sample and they were summed, calibrated, background subtracted, and normalized using Athena.[18]

Electrochemical measurement.—Electrodes were prepared by making slurries containing 80 wt% active cathode material, 10 wt% polyvinylidene fluoride (PVDF) binder, and 10 wt% Carbon Super P. All the preparation was carried out in an Ar-filled glovebox and these electrodes were then incorporated into 2032 electrochemical cells using a Li metal as counter electrode, the Whatman glass fibre as separators and 1 M LiPF6 in 1:1 w/w ethylene carbonate—dimethyl carbonate as electrolyte. Electrochemical measurements were performed using a Maccor battery cycler at room temperature. The charge and discharge experiments were carried out galvanostatically at a constant current over a voltage range 2.0 to 4.3 V and 2.0 to 4.8 V.

Results and Discussion

Structural and morphological characterization.—Li_2NiO_2F was synthesized as described in the Experimental section. Powder X-ray Diffraction (PXRD), Supplementary Fig. 1 (available online at stacks.iop.org/JES/168/080521/mmedia), confirmed $LiNiO_2$ was a single phase precursor and with a stoichiometry $Li_{0.98}Ni_{1.02}O_2$ (molar volume = 33.86(1) A^3) according to the interrelation between composition and the Rhombohedral unit cell volume, Table SI.[19] The ball-milling reaction was performed under Argon atmosphere in hermetically sealed jars and no pressurisation of the jar from O_2 release during milling was observed implying a lack of change in Ni oxidation state from $LiNiO_2$ to Li_2NiO_2F. The Li:Ni atomic ratio in the as-prepared Li_2NiO_2F was also measured by Inductively Coupled Plasma—Optical Emission Spectroscopy (ICP-OES), and is in close agreement Supplementary Table SI. Energy-dispersive spectroscopy (EDS) mapping images, presented in Supplementary Fig. 2 confirm the uniform distribution of Ni, O and F throughout the particles.

PXRD data were collected on the pristine Li_2NiO_2F, Fig. 1, and can be indexed on the rocksalt structure, space group *Fm*-3*m*, without the presence of crystalline impurity phases. Li_2NiO_2F exhibits very broad peaks, common to rocksalts prepared by ball-milling. Reitveld refinement was carried out yielding a lattice parameter of 4.0748(2) Å, which is smaller than for the Mn-analogue Li_2MnO_2F (4.1176(5) Å) in line with the differences in the ionic radii of Ni^{3+} and Mn^{3+}.[7] The lattice and structural parameters are presented in Supplementary Table SIII.

The morphology of the ball-milled particles was examined using scanning electron microscopy (SEM), Supplementary Fig. 3, revealing secondary particle sizes in the range 50–200 nm. Selected area electron diffraction (SAED) data, Fig. 2a, show reflections that can be indexed on a cubic *Fm*-3*m* cation-disordered rock-salt. High-resolution transmission electron microscopy (HRTEM) images, Fig. 2b, show that the secondary particles are composed of smaller primary particles about 5–10 nm in size, in line with the broad X-ray diffraction peaks seen in Fig. 1. The lattice fringes with interplanar spacing 0.20 nm are also shown corresponding to the (200) plane of Li_2NiO_2F rocksalt structure.

^{6}Li and ^{19}F solid-state magic angle spinning (MAS) NMR spectroscopy were performed to investigate lithium and fluorine within Li_2NiO_2F, Fig. 3. The ^{6}Li spectrum for $LiNiO_2$ shows a single resonance centred at ∼710 ppm corresponding to Li in the alkali layer, consistent with previous reports and confirming the purity of the precursor.[20] In the Li_2NiO_2F disordered rocksalt, the main resonance is at a significantly lower chemical shift, with a centre of gravity closer to ∼30 ppm. This is due partly to the increased lithium content which dilutes the number of neighbouring paramagnetic Ni centres but also indicates a substantial degree of disorder. The asymmetric tail arises from different local Li environments with varying proximity to Ni, characteristic of disordered rocksalts.[21] The environments at higher chemical shifts are surrounded by a greater number of paramagnetic Ni^{3+} centres. Likewise, a similar peak asymmetry is observed in the ^{19}F NMR spectrum of Li_2NiO_2F, which also shows a tail away from the LiF isotropic chemical shift (−204 ppm). These observations indicate successful bulk incorporation of Li and F into the disordered rock salt lattice.

Electrochemical characterization.—First-cycle charge and discharge curves of Li_2NiO_2F between 2−4.8 V are shown in Fig. 4a. Li_2NiO_2F exhibits a first charge capacity of 300 mAh g^{-1} (equivalent to 1.38 li per formula unit), 80 mAh g^{-1} beyond the theoretical capacity of 220 mAh g^{-1} based on oxidation of Ni^{3+} to Ni^{4+}. However, this is not completely recovered on discharge and almost 100 mAh g^{-1} of irreversible capacity is observed. After the initial charge-discharge, the material exhibits decreasing capacity over subsequent cycles (Fig. 4b and Supplementary Fig. S5). Limiting the upper voltage cut-off to 4.3 V avoids the irreversible capacity loss and improves the subsequent capacity decay, consistent with the charge stored above this voltage limit being irreversible in nature, Figs. 4c, 4d and Supplementary Fig. S5.

On discharging from 4.3 V to 2.0 V, there is evidence of a small amount of excess capacity which most likely arises from lithiation of cation vacancy defects. To check for cation vacancies in the pristine material, we discharged the pristine material to 2 V and observed 50 mAh g^{-1} capacity (equivalent to 0.25 li), Supplementary Fig. S6. The low voltage of this capacity is consistent with the accompanying reduction of Ni from +3 to +2, implying there must be some anion as well as cation vacancies in pristine Li_2NiO_2F.

Charge compensation in Li_2NiO_2F.—Oxygen loss is a common mechanism of irreversible capacity in cathode materials at high voltages. To quantify the amount of oxygen loss from Li_2NiO_2F, operando electrochemical mass spectrometry (OEMS) was employed. The OEMS results are presented in Fig. 5 and show a significant amount of O_2 and CO_2 released during the initial charge. Quantification of the evolved gases reveals up to 120 mAh g^{-1} of capacity can be attributed to O loss through direct O_2 evolution and CO_2 from oxygen releases from the lattice reacting with the electrolyte. Analysis of the latter followed the previously described procedure.[22] After the first cycle, the amount of O loss is much diminished and correspondingly there is improved capacity retention. Similarly, by limiting the first cycle voltage cut-off to 4.3 V,

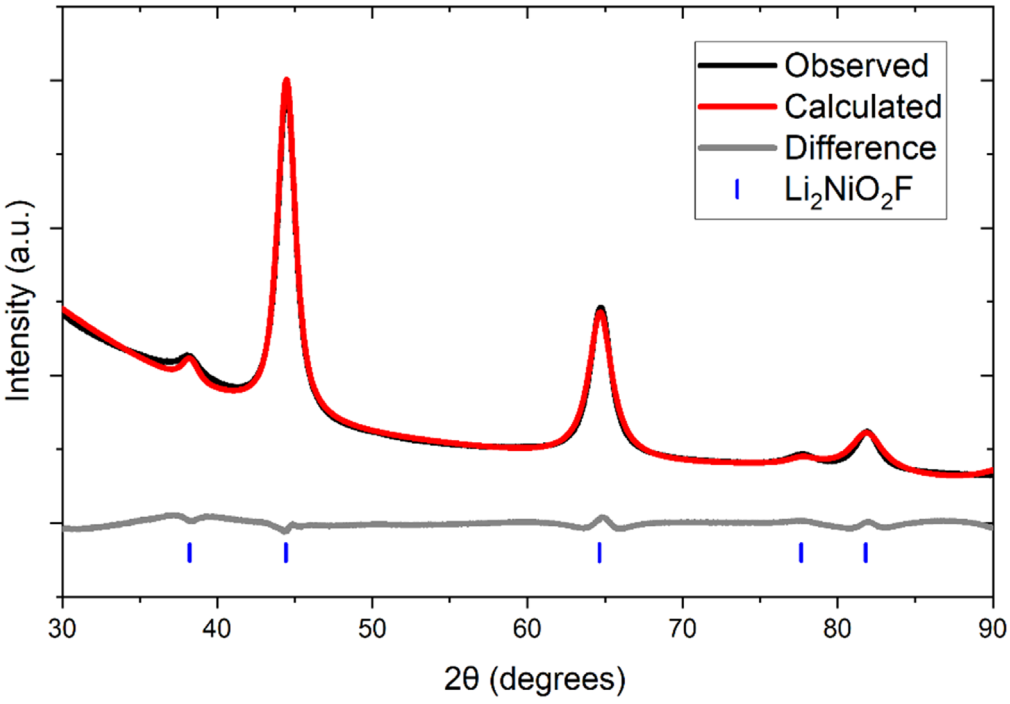

Figure 1. Rietveld refinement result of powder X-ray diffraction data for Li_2NiO_2F in the Fm-3m space group and yielding a unit cell parameter of 4.0748(2) A.

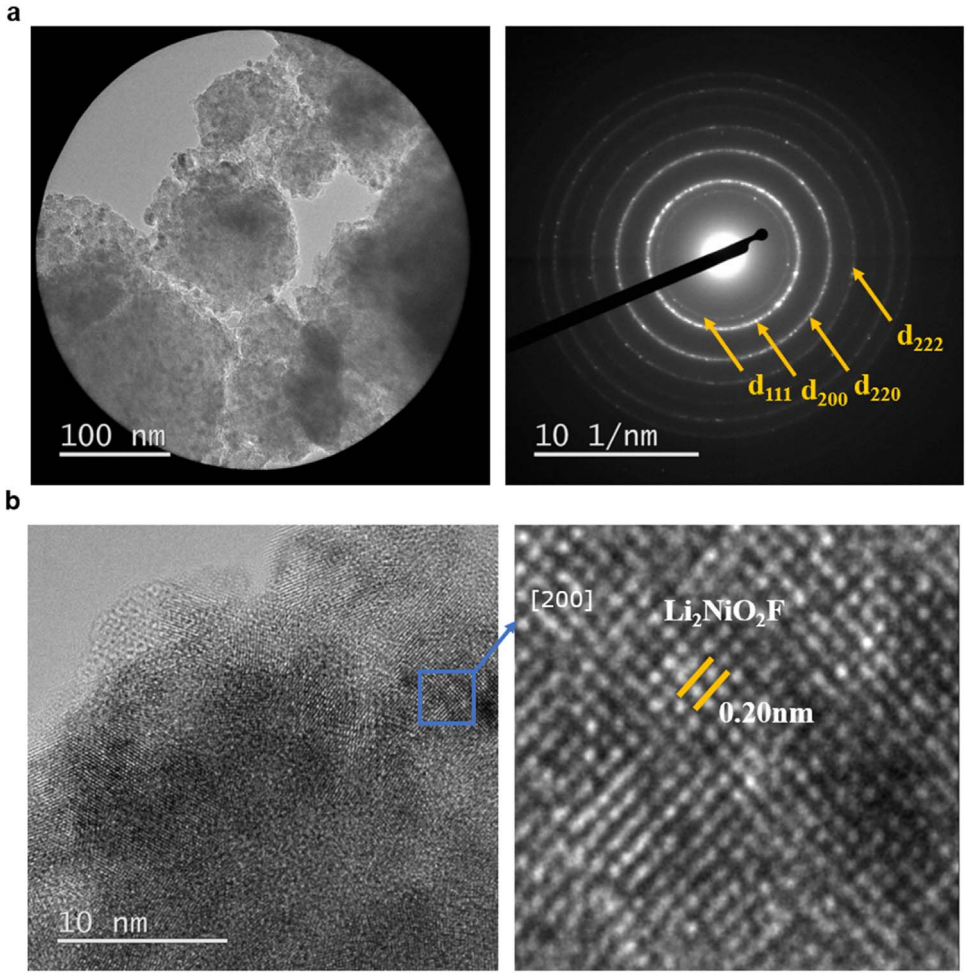

Figure 2. (a) SAED patterns of the Li_2NiO_2F, with indexing of the diffraction ring showing rock-salt *Fm-3m* structure; (b) HR-TEM images of Li_2NiO_2F.

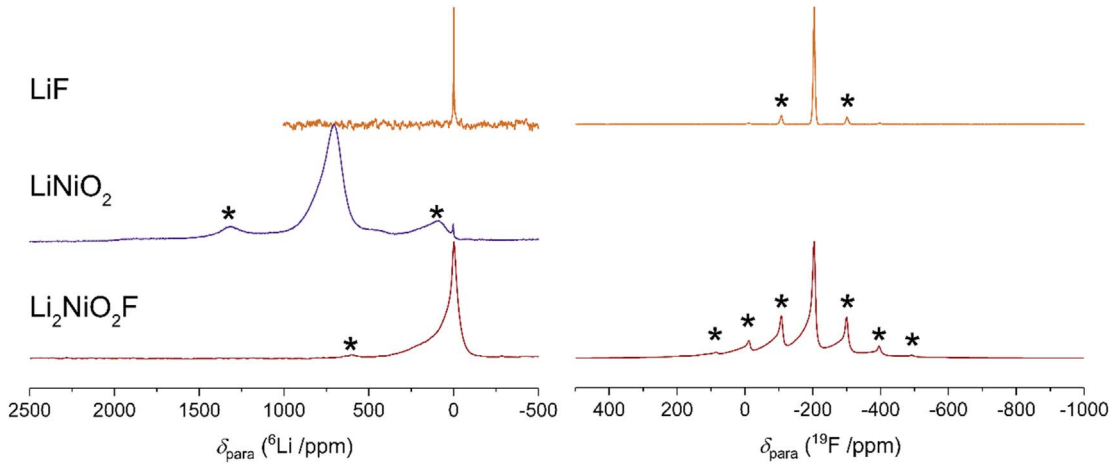

Figure 3. The ^{6}Li (left panel) and ^{19}F (right panel) solid state MAS NMR spectra for the precursors (LiF and $LiNiO_2$) and the as prepared Li_2NiO_2F. Asterisks denote the spinning sidebands.

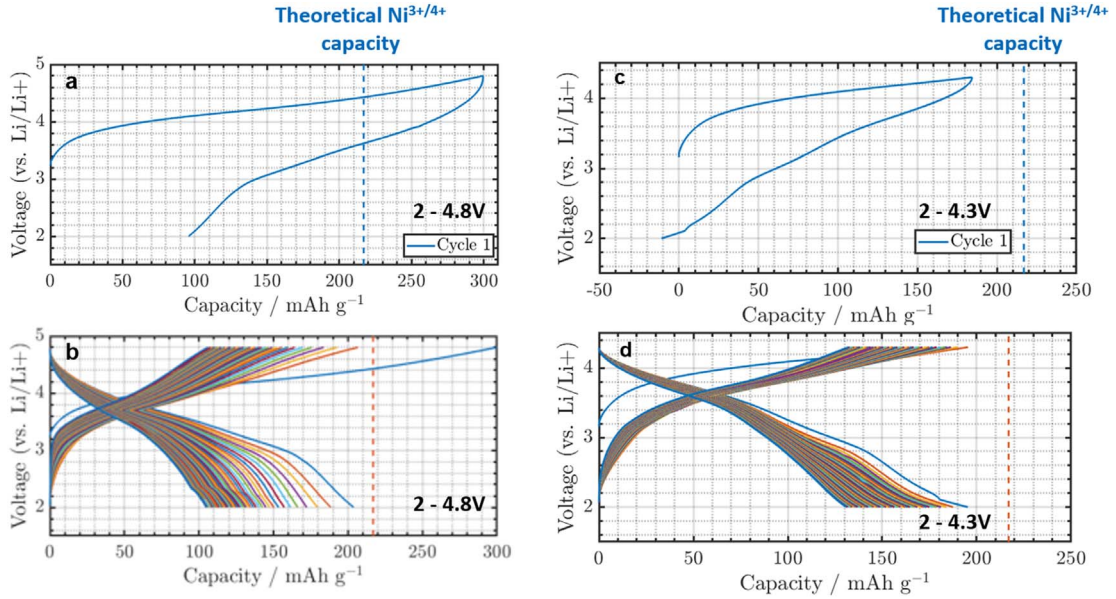

Figure 4. Galvanostatic charge and discharge profiles for Li_2NiO_2F (a) first cycle between 2.0 and 4.8 V. (b) Up to 50 cycles between 2.0 and 4.8 V. (c) first cycle between 2.0 and 4.3 V. (d) Up to 50 cycles between 2.0 and 4.3 V. The dashed lines represent the theoretical capacity based on $Ni^{3+/4+}$ redox in the sample.

which is before most of the O loss is observed, there is significantly less irreversible capacity.

To investigate the redox changes on Ni accompanying the first cycle, K-edge XANES data were collected, Supplementary Fig. S4. On charge, there is an increase in the main edge energy indicating Ni oxidises towards +4. On discharge, the main edge shifts to a lower energy than that of the pristine indicating Ni is reduced below the initial +3 state. After discharging to 2 V, the XANES data appear to show a greater degree of Ni reduction than that expected electrochemically accounting for the irreversible capacity from O loss (200 mAh g^{-1} discharge capacity and 300–120 = 180 mAh g^{-1} reversible charge capacity). This implies that some of the oxygen loss arises from Ni reduction at the surface (i.e. through reductive elimination $2Ni^{4+}–O^{2-} \rightarrow 2Ni^{2+} + O_2$) rather than direct oxidation of the oxide ions.

Discussion.—Li_2NiO_2F is a new addition to the expanding family of archetypal Li_2TMO_2F oxyfluoride disordered rocksalt compounds. Compared with the other oxyfluoride analogues such as Li_2MnO_2F, Li_2NiO_2F exhibits a considerable degree of first cycle O loss and irreversible capacity when charged to 4.8 V. After the first cycle, the amount of O loss is much smaller and the irreversible capacity over subsequent charge and discharge cycles is consequently much less pronounced. The continuous capacity fade over cycling that is observed in Li_2NiO_2F, even when O loss is suppressed by limiting the upper cut-off voltage to 4.3 V, is a common characteristic of the disordered rocksalt materials in general. The origin of this capacity fade issue has been linked to metal dissolution. Yabuuchi et al. recently demonstrated for $Li_{2.1}Mo_{0.7}Ti_{0.2}O_2F$ that significant improvement in capacity retention can be realised by suppressing metal dissolution.[23] To assess the role of metal dissolution in Li_2NiO_2F, we performed elemental analysis on the cathode after cycling using ICP-OES. The results show a loss of 2.5% of the Ni from the cathode after 100 cycles, Supplementary Fig. S7, indicating dissolution does contribute in part to the gradual capacity decay that is seen. This degree of dissolution is less pronounced than the Mn rocksalt analogue where we detected 8% loss of Mn after 100 cycles, which is in line with broader understanding that Mn dissolution tends to be more severe than Ni in other cathodes, such as the layered oxides and Li-rich materials.[24] Given the extent of the capacity decay we observe for Li_2NiO_2F (almost 50% loss by 50 cycles) we conclude that this small amount

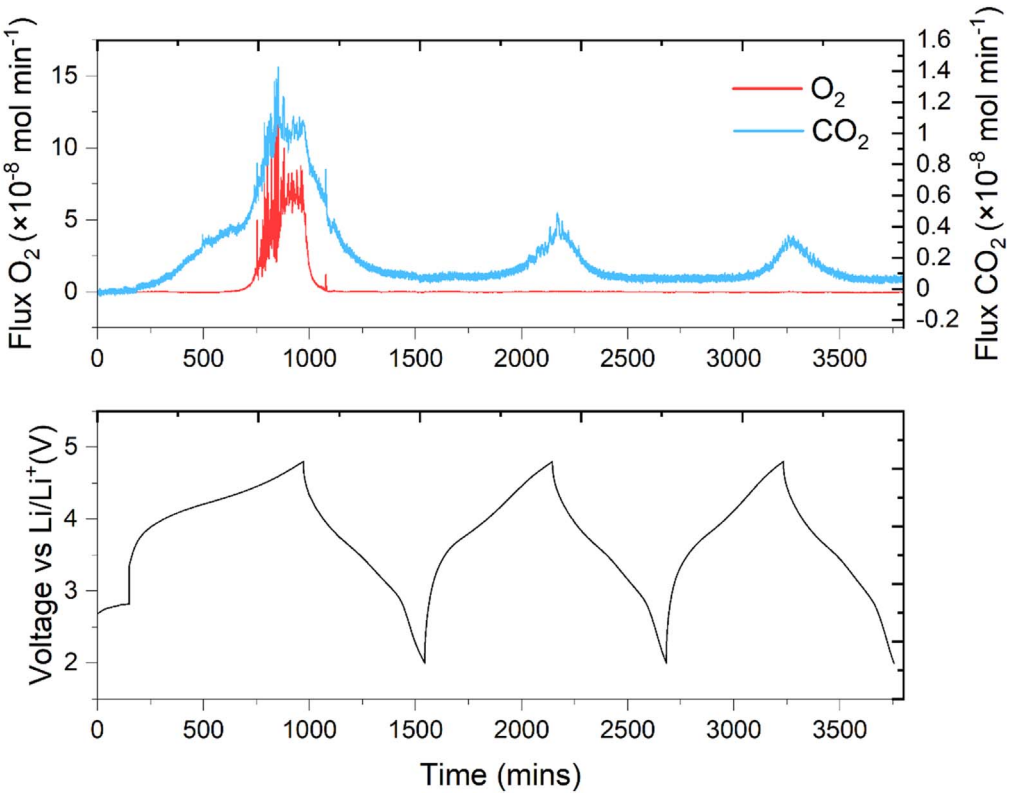

Figure 5. Operando electrochemical mass spectrometry (OEMS) conducted on the first three cycles of Li_2NiO_2F. Extensive O-loss is observed in the form of O_2 and CO_2 during the first charge.

of dissolution is unlikely to be the dominant process responsible here and instead more complex surface instability or interphase formation are likely to be the cause. Future work targeted at understanding and inhibiting these surface reactions which affect all disordered rocksalts, will help improve the performance of these new materials.

Conclusions

We report the synthesis and characterisation of a new disordered rocksalt oxyfluoride compound, Li_2NiO_2F, the first based on Ni. The structure and morphology of Li_2NiO_2F conforms to other rocksalt materials prepared by mechanochemical ball-milling with 5–10 nm primary crystallite sizes. Li_2NiO_2F can store 300 mAh g^{-1} capacity on charge up to 4.8 V of which 120 mAh g^{-1} is attributed to irreversible O-loss leading to a discharge capacity of 200 mAh g^{-1} at an average voltage of 3.2 V. Li_2NiO_2F would be a promising Co-free cathode if strategies to suppress O loss and capacity fade over cycling could be successfully implemented.

Acknowledgments

P.G.B. is indebted to the EPSRC, the Henry Royce Institute for Advanced Materials (EP/R00661X/1, EP/S019367/1 and EP/R010145/1) and the Faraday Institution (FIRG007 and FIRG008) for financial support. The authors gratefully acknowledge the team at B18, Diamond Light Source for their assistance collecting XANES data through the Energy Materials Block Allocation Group.

ORCID

John-Joseph Marie https://orcid.org/0000-0003-3004-199X
Gregory J. Rees https://orcid.org/0000-0002-7514-1516
Robert A. House https://orcid.org/0000-0002-7415-477X
Peter G. Bruce https://orcid.org/0000-0001-6748-3084

References

1. M. Freire et al., "A new active Li-Mn-O compound for high energy density Li-ion batteries." *Nat. Mater.*, **15**, 173 (2015).
2. R. Wang et al., "A disordered rock-salt Li-excess cathode material with high capacity and substantial oxygen redox activity: $Li_{1.25}Nb_{0.25}Mn_{0.5}O_2$." *Electrochem. Commun.*, **60**, 70 (2015).
3. N. Yabuuchi et al., "Origin of stabilization and destabilization in solid-state redox reaction of oxide ions for lithium-ion batteries." *Nat. Commun.*, **7**, 13814 (2016).
4. J. Lee et al., "Unlocking the potential of cation-disordered oxides for rechargeable lithium batteries." *Science*, **343**, 519 (2014).
5. A. Urban, J. Lee, and G. Ceder, "The configurational space of rocksalt-type oxides for high-capacity lithium battery electrodes." *Adv. Energy Mater.*, **4**, 1400478 (2014).
6. R. Chen et al., "Disordered lithium-rich oxyfluoride as a stable host for enhanced Li + intercalation storage." *Adv. Energy Mater.*, **5**, 1401814 (2015).
7. R. A. House et al., "Lithium manganese oxyfluoride as a new cathode material exhibiting oxygen redox." *Energy\& Environ. Sci.*, **11**, 926 (2018).
8. R. Sharpe et al., "Redox chemistry and the role of trapped molecular O_2 in Li-rich disordered rocksalt oxyfluoride cathodes." *J. Am. Chem. Soc.*, **142**, 21799 (2020).
9. J. M. Ateba Mba et al., "Ceramic synthesis of disordered lithium rich oxyfluoride materials." *J. Power Sources*, **467**, 228230 (2020).
10. J.-M. A. Mba et al., "Ceramic synthesis of disordered lithium rich oxyfluoride and the impact of their defects in electrochemical performances." *ECS Meet. Abstr*, **MA2019-01**, 62 (2019).
11. N. Takeda et al., "Reversible Li storage for nanosize cation/anion-disordered rocksalt-type oxyfluorides: $LiMoO_2$-xLiF ($0 \leqslant x \leqslant 2$) binary system." *J. Power Sources*, **367**, 122 (2017).
12. D. A. Kitchaev et al., "Design principles for high transition metal capacity in disordered rocksalt Li-ion cathodes." *Energy Environ. Sci.*, **11**, 2159 (2018).
13. J. Lee et al., "Reversible Mn^{2+}/Mn^{4+} double redox in lithium-excess cathode materials." *Nat.*, *2018 5567700***556**, 185 (2018).
14. Y. Tomita et al., "Synthesis and electrochemical properties of 4LiF-$NiMn_2O_4$ composite as a cathode material for Li-ion batteries." *J. Power Sources*, **354**, 34 (2017).
15. N. Yabuuchi et al., "High-capacity electrode materials for rechargeable lithium batteries: Li_3NbO_4-based system with cation-disordered rocksalt structure." *Proc. Natl. Acad. Sci. U. S. A.*, **112**, 7650 (2015).
16. H. Ji et al., "Computational Investigation and experimental realization of disordered high-capacity li-ion cathodes based on Ni redox." *Chem. Mater.*, **31**, 2431 (2019).
17. A. J. Dent et al., "B18: a core XAS spectroscopy beamline for diamond." *J. Phys. Conf. Ser.*, **190**, 012039 (2009).

18. B. Ravel and M. Newville, "Athena, artemis, hephaestus: data analysis for X-ray absorption spectroscopy using IFEFFIT." *J. Synchrotron Radiat.*, **12**, 537 (2005), (International Union of Crystallography (IUCr).
19. J. R. Dahn, U. von Sacken, and C. A. Michal, "Structure and electrochemistry of $Li_{1\pm y}NiO_2$ and a new Li_2NiO_2 phase with the $Ni(OH)_2$ structure." *Solid State Ionics*, **44**, 87 (1990).
20. C. Chazel, M. Ménétrier, L. Croguennec, and C. Delmas, "$^{6/7}$Li NMR study of the $Li_{1-z}Ni_{1+z}O_2$ phases." *Magn. Reson. Chem.*, **43**, 849 (2005).
21. F. Geng et al., "Anionic redox reactions and structural degradation in a cation-disordered rock-salt $Li_{1.2}Ti_{0.4}Mn_{0.4}O_2$ cathode material revealed by solid-state NMR and EPR." *J. Mater. Chem. A*, **8**, 16515 (2020).
22. K. Luo et al., "Charge-compensation in 3d-transition-metal-oxide intercalation cathodes through the generation of localized electron holes on oxygen." *Nat. Chem.*, **8**, 684 (2016).
23. N. Takeda, I. Ikeuchi, R. Natsui, K. Nakura, and N. Yabuuchi, "Improved electrode performance of lithium-excess molybdenum oxyfluoride: titanium substitution with concentrated electrolyte." *ACS Appl. Energy Mater.*, **2**, 1629 (2019).
24. C. Zhan, T. Wu, J. Lu, and K. Amine, "Dissolution, migration, and deposition of transition metal ions in Li-ion batteries exemplified by Mn-based cathodes—a critical review." *Energy Environ. Sci.*, **11**, 243 (2018).